

Semi-preservation of momentum and heat transfer in cascade-wake-flows

J. W. ELSNER and J. ZIELIŃSKI

Thermal Machinery Institute, Technical University of Częstochowa, Deglera 35, 42-200 Częstochowa, Poland

(Received 2 July 1984 and in final form 9 August 1985)

Abstract—The paper presents the idea of semi-preservation in nonisothermal cascade-wake-flows. In contrast with the self-similarity concept, the evolution of semi-preserving flows is described in terms of characteristic velocity and temperature scales, separate for the mean and turbulent motion. Transport equations, of momentum and heat allow one to deduce the mutual correlations between individual scales and to derive a simple formula for turbulent Prandtl number, expressing Pr_T in terms of mean-flow parameters only. Finally, the theoretical predictions are confronted with authors' own experimental data.

1. INTRODUCTION

THE processes of heat and mass transfer as well as the evolution of a turbulent flow pattern behind a row of heated symmetrical bodies have been the object of great interest both from the theoretical and practical point of view. The development of the subject can be traced in a number of papers and scientific reports. This problem was probably undertaken for the first time in 1936 by Gran Olsson [1] who, on the basis of Prandtl's mixing-length theory, derived the relationships describing the mean-flow evolution in the absence of a longitudinal pressure gradient. His measurements, confined to the mean quantities only, pointed out that velocity defect as well as temperature excess decayed in the downstream direction at a rate inversely proportional to the streamwise coordinate x_1 .

The turbulent flow pattern behind a row of parallel rods was also studied by Sato [2] as well as by Tamaki and Oshima [3] in the early 1950s. The empirical data obtained by Sato revealed that turbulence energy decayed in the downstream direction according to the power-law dependence upon the streamwise coordinate x_1 , with the power indices increasing monotonously with the frequency of turbulent eddies. On the other hand the eddy viscosity coefficient ν_T was found to be nearly constant in all cross-sections of the flow, increasing slightly with the distance from the rods.

On the contrary, Tamaki and Oshima in their experiment found ν_T to be a decreasing function of coordinate x_1 , approximately according to the relation $\nu_T \sim x_1^{-1}$. A similar conclusion was drawn by Klatt [4], who stated that eddy viscosity coefficient appeared to be the decaying power function of the distance from the grid.

Evolution of Reynolds stresses and eddy viscosity behind the row of symmetrical bodies in a wake-flow with constant longitudinal pressure gradient has been analysed by Elsner and Wilczyński [5, 6]. They have pointed out that the positive value of $\partial p / \partial x_1$ causes the

growth of the overall turbulence level, while the negative pressure gradient accelerates the mean velocity field equalization and suppresses the turbulent fluctuations of the flowing medium. According to [6], the eddy viscosity coefficient ν_T decreases considerably in the downstream direction and in the far-flow region it appears to be an increasing function of the longitudinal pressure gradient.

A similar type of flow was analysed experimentally by Matsui [7] who found that when the row-pitch to rod-diameter ratio became sufficiently small, the mean velocity and temperature profiles lost their usual periodicity.

The problem of turbulent heat transfer and its dependence upon turbulence macroscales was investigated by Kühn [8] in 2D flows behind the grid of bars with several specially collocated heat sources, consisting of fine, electrically heated wires. The experiment pointed out that the eddy conductivity increased with the growth of turbulence macroscales as well as with the intensity of velocity fluctuations. Similar studies were also carried out by Kühn [9] four years later in a flow behind an oscillating grid where the macroscales as well as the rate of heat spread were considerably higher than those in usual flows behind the stationary grids.

For the first time the idea of semi-preservation in an isothermal cascade-wake-flow has been formulated by Elsner [10]. In contrast with the self-similarity hypothesis, which is too well known to need further description, the idea of semi-preservation assumes that the overall flow pattern at a certain distance behind the cascade of symmetrical bodies may be described by means of two velocity scales, different for the mean and turbulent motion and decreasing according to a power law in the downstream direction.

The main purpose of this report is to extend the semi-preservation idea over the processes of turbulent heat transfer in nonisothermal cascade-wake-flows. We particularly focused our attention on the evolution of eddy diffusion coefficients for momentum and heat,

NOMENCLATURE

a_T coefficient of turbulent heat diffusion
 $F, F_\Theta, f_{12}, f_i, f_\vartheta, f_{2\vartheta}$ semi-preservation functions defined by equation (9)
 H flow overheat parameter defined by equation (20)
 $k_i, k_\vartheta, k_{12}, k_{2\vartheta}$ exponent indices in equation (15)
 Pr_T turbulent Prandtl number
 $R_{12}, R_{2\vartheta}$ correlation coefficients defined by equation (10)
 $s_{12}, s_{2\vartheta}$ exponent indices in equation (15)
 t cascade pitch (Fig. 1)
 U_1 streamwise component of mean velocity
 U_M, U_{av} average values of mean velocity according to equations (1) and (21), respectively
 U^*, u^* mean and fluctuating velocity scales
 u_i fluctuating velocity in x_i direction
 x_i Cartesian coordinates.

Greek symbols
 η relative coordinate
 Θ mean temperature
 Θ_M, Θ_{av} average values of mean temperature according to equations (2) and (21), respectively
 Θ^*, ϑ^* mean and fluctuating temperature scales
 ϑ fluctuating temperature
 κ, κ_Θ exponential indices in equation (15)
 ν_T coefficient of eddy viscosity.

Other symbols
 $'$ denotes derivative with respect to the relative coordinate $\eta = x_2/t$
 $-$ denotes the time average values of turbulent quantities.

respectively, in order to check the behaviour of turbulent Prandtl number in this type of flow.

2. SEMI-PRESERVATION OF NONISOTHERMAL CASCADE-WAKE-FLOW

The theoretical approach to the evolution of both the velocity and temperature fields behind a row of slightly heated flat plates (Fig. 1) may be considerably simplified by the assumption that the amount of heat supplied to the fluid is too small to affect the dynamics of the flow. Under such circumstances it seems reasonable to expect that the variation of fluid density in the whole flow region can also be neglected which allows the introduction of the reference values of velocity U_M and

temperature Θ_M , averaged over the cascade pitch t according to the relationships

$$U_M = \frac{1}{t} \int_0^t U_1(x_1, x_2) dx_2 = \text{const} \quad (1)$$

$$\Theta_M = \frac{1}{t U_M} \int_0^t \Theta(x_1, x_2) U_1(x_1, x_2) dx_2 = \text{const.} \quad (2)$$

At a sufficient distance behind the plates, in the region of uniform static pressure, the equations of turbulent motion and heat transfer may be written in a simplified form

$$U_1 \frac{\partial U_1}{\partial x_1} + \frac{\partial}{\partial x_2} \overline{u_1 u_2} = 0 \quad (3)$$

$$U_1 \frac{\partial \Theta}{\partial x_1} + \frac{\partial}{\partial x_2} \overline{u_2 \vartheta} = 0. \quad (4)$$

Taking advantage of the Boussinesq concept and expressing correlations $\overline{u_1 u_2}$ and $\overline{u_2 \vartheta}$ in terms of eddy diffusion coefficients

$$\nu_T = \frac{-\overline{u_1 u_2}}{\partial U_1 / \partial x_2} \quad (5)$$

$$a_T = \frac{-\overline{u_2 \vartheta}}{\partial \Theta / \partial x_2} \quad (6)$$

which, according to numerous opinions [2, 3, 5, 6], are supposed to have constant values in the x_2 -direction, it is convenient to rewrite equation (3) and (4) in the form

$$U_1 \frac{\partial U_1}{\partial x_1} - \nu_T \frac{\partial^2 U_1}{\partial x_2^2} = 0 \quad (7)$$

$$U_1 \frac{\partial \Theta}{\partial x_1} - a_T \frac{\partial^2 \Theta}{\partial x_2^2} = 0. \quad (8)$$

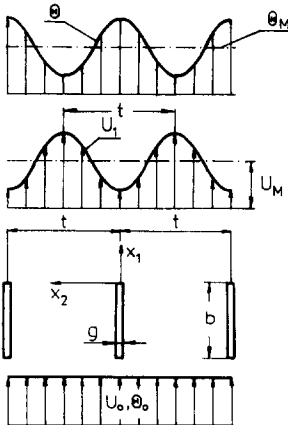


FIG. 1. The schematic sketch of mean velocity and temperature profiles.

Let us assume that the type of flow considered develops in a semi-preserving mode in which the overall flow pattern may be described by means of two velocity (U^* , u^*) and two temperature (Θ^* , ϑ^*) scales, different for the mean (U^* , Θ^*) and turbulent (u^* , ϑ^*) motions. The semi-preserving relations utilizing the nondimensional functions F and f of the relative coordinate $\eta = x_2/t$ can be formulated as

$$\begin{aligned} U_1(x_1, x_2) &= U_M - U^*(x_1)F(\eta) \\ \overline{u_1^2}(x_1, x_2) &= u^{*2}(x_1)f_1(\eta) \\ \overline{u_1 u_2}(x_1, x_2) &= R_{12}^*(x_1)u^{*2}(x_1)f_{12}(\eta) \\ \Theta(x_1, x_2) &= \Theta_M + \Theta^*(x_1)F_\Theta(\eta) \\ \overline{\vartheta^2}(x_1, x_2) &= \vartheta^{*2}(x_1)f_\vartheta(\eta) \\ \overline{u_2 \vartheta}(x_1, x_2) &= R_{2\vartheta}^*(x_1)u^*(x_1)\vartheta^*(x_1)f_{2\vartheta}(\eta). \end{aligned} \quad (9)$$

where the symbols R_{12}^* and $R_{2\vartheta}^*$ designate the maximum values of the correlation coefficients

$$R_{12}(x_1, x_2) = \frac{\overline{u_1 u_2}}{(\overline{u_1^2} \overline{u_2^2})^{1/2}} = R_{12}^*(x_1)F_R(\eta) \quad (10a)$$

$$R_{2\vartheta}(x_1, x_2) = \frac{\overline{u_2 \vartheta}}{(\overline{u_2^2} \overline{\vartheta^2})} = R_{2\vartheta}^*(x_1)f_R(\eta). \quad (10b)$$

Now, if relations (9) are introduced into equations (3) and (4) or (7) and (8), respectively, and furthermore, if we assume that at a sufficient distance behind the plates

$$U^*/U_M \ll 1; \quad \Theta^*/\Theta_M \ll 1$$

then, after neglecting the quantities of the second order, we obtain

$$\frac{tU_M}{R_{12}^* u^{*2}} \frac{dU^*}{dx_1} = \frac{f'_{12}}{F} = c_1 \quad (11a)$$

$$\frac{tU_M}{R_{2\vartheta}^* u^* \vartheta^*} \frac{d\Theta^*}{dx_1} = \frac{-f'_{2\vartheta}}{F_\Theta} = c_2 \quad (11b)$$

and respectively

$$\frac{t^2 U_M}{v_T U^*} \frac{dU^*}{dx_1} = \frac{F''}{F} = c_3 \quad (12a)$$

$$\frac{t^2 U_M}{a_T \Theta^*} \frac{d\Theta^*}{dx_1} = \frac{F''_\Theta}{F_\Theta} = c_4. \quad (12b)$$

The area in which equations (11) and (12) are fulfilled for any arbitrarily chosen values of coordinates x_1 and x_2 has been called the 'semi-preserving' region of an nonisothermal cascade-wake-flow [10].

Assuming $c_3 = c_4 = -4\pi^2$ one can easily obtain from equations (11) and (12) the formulae

$$F(\eta) = F_\Theta(\eta) = \cos 2\pi\eta \quad (13)$$

$$f_{12}(\eta) = \frac{c_1}{2\pi} \sin 2\pi\eta \quad (14a)$$

$$f_{2\vartheta}(\eta) = \frac{-c_2}{2\pi} \sin 2\pi\eta \quad (14b)$$

describing the lateral distributions of the quantities U_1 , Θ , $\overline{u_1 u_2}$ and $\overline{u_2 \vartheta}$ in a semi-preserving region of flow.

Following the experimental evidence let us assume that at a certain distance $x_1 > x_{10}$ all the quantities appearing in Equations (9) and (10) show the power-law dependence upon the streamwise coordinate $x_1 - a$, where a determines the position of virtual origin of flow. Without loss of generality the value of a will be put to zero so that the functional relationships considered before may be expressed in the form

$$\left. \begin{aligned} \frac{U^*}{U_0^*} &= \left(\frac{x_1}{x_{10}}\right)^{-\kappa} & \frac{u^*}{u_0^*} &= \left(\frac{x_1}{x_{10}}\right)^{-k} \\ \frac{\overline{u_1 u_2}}{(\overline{u_1 u_2})_0} &= \left(\frac{x_1}{x_{10}}\right)^{-k_{12}} & \frac{R_{12}^*}{(R_{12}^*)_0} &= \left(\frac{x_1}{x_{10}}\right)^{-s_{12}} \\ \frac{\Theta^*}{\Theta_0^*} &= \left(\frac{x_1}{x_{10}}\right)^{-\kappa_\Theta} & \frac{\vartheta^*}{\vartheta_0^*} &= \left(\frac{x_1}{x_{10}}\right)^{-k_\vartheta} \\ \frac{\overline{u_2 \vartheta}}{(\overline{u_2 \vartheta})_0} &= \left(\frac{x_1}{x_{10}}\right)^{-k_{2\vartheta}} & \frac{R_{2\vartheta}^*}{(R_{2\vartheta}^*)_0} &= \left(\frac{x_1}{x_{10}}\right)^{-s_{2\vartheta}} \end{aligned} \right\} \quad (15)$$

where the subscript 0 denotes the values attributed to the coordinate x_{10} .

Substituting the above relations in equations (10) and (11) we are able to ascertain the additional correlations between individual power indices

$$\begin{aligned} k_{12} &= \kappa + 1; & k_{2\vartheta} &= \kappa_\Theta + 1 \\ s_{12} &= \kappa + 1 - 2k; & s_{2\vartheta} &= \kappa_\Theta + 1 - (k + k_\vartheta). \end{aligned} \quad (16)$$

Because of a general tendency towards the stabilization of isotropic structure observed in majority of free turbulent flows, both the correlation coefficients R_{12} and $R_{2\vartheta}$ should decay along the coordinate x_1 , hence

$$\kappa + 1 = k_{12} > 2k; \quad \kappa_\Theta + 1 = k_{2\vartheta} > k + k_\vartheta. \quad (17)$$

It is worth keeping in mind that the assumption of self-similarity immediately gives $\kappa = \kappa_\Theta = k = k_\vartheta = 1$, which corresponds to the constant values of correlation coefficients R_{12} and $R_{2\vartheta}$ ($s_{12} = s_{2\vartheta} = 0$) in the downstream direction.

On the other hand, when equations (11) and (15) are combined, both eddy transport coefficients v_T and a_T appear to be inversely proportional to the streamwise coordinate x_1 , according to the formulae

$$\begin{aligned} v_T &= \frac{\kappa U_M t^2}{4\pi^2} \frac{1}{x_1} \\ a_T &= \frac{\kappa_\Theta U_M t^2}{4\pi^2} \frac{1}{x_1} \end{aligned} \quad (18)$$

which imply the constant value of the turbulent Prandtl number

$$Pr = \frac{v_T}{a_T} = \frac{\kappa}{\kappa_\Theta}. \quad (19)$$

The relations derived above clearly show that in order to evaluate the quantities v_T , a_T and Pr_T there is no need to measure the correlations $\overline{u_1 u_2}$ and $\overline{u_2 \vartheta}$ but it is quite enough to determine the evolution of mean velocity and temperature fields.

3. EXPERIMENTAL APPARATUS AND PROCEDURE

In order to check the validity of the semi-preservation idea outlined in the previous section, a set of the experimental investigations has been performed in a low-speed open circuit wind tunnel shown schematically in Fig. 2. The tested cascade consisted of five electrically heated metal plates having width $b = 80$ mm, thickness $g = 10$ mm, length $l = 200$ mm (measured in the x_3 -direction) and spaced (see Fig. 1) at a distance $t = 55$ mm from one another.

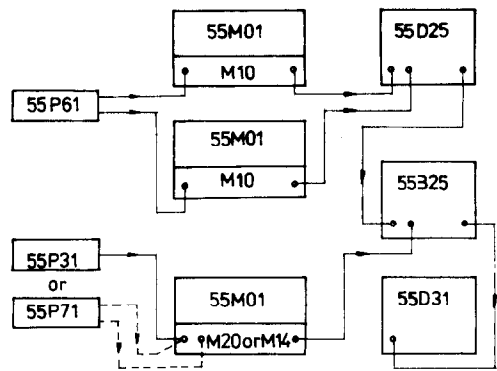
The flexible top and bottom walls of the measuring section could be suitably adjusted in order to compensate for the longitudinal increase of the end-wall boundary-layer thickness and to fulfill the conditions $p(x_1) = \text{const}$ and $t(x_1) = \text{const}$ (see Fig. 1). The traversing mechanism mounted on the upper wall (Fig. 2) allowed the probes to move in the x_2 -direction with an accuracy up to 0.01 mm.

The mean temperature and velocity fields were determined respectively by means of a thermistor with digital readout and a Pitot tube, with the accuracy of the pressure reading about 0.7 Pa. The measurements of the turbulent quantities such as Reynolds stresses, temperature variance and velocity-temperature correlation were carried out by means of a three-channel DISA 55M System hot-wire anemometer. The block diagram of the setups used for measurements of particular turbulent quantities are shown in Fig. 3. During the experiment the following DISA-sensors were applied: x -probe type 55P61, temperature compensated probe 55P71 and resistance thermometer 55P31.

In the course of investigations the amount of heat transferred to the flowing medium was controlled by the value of the electric current supplied to the plates. For the quantitative estimation of this heat flux, the notion of the 'flow-overheat' parameter has been introduced

$$H = \frac{N/l \cdot t}{\rho U_M c_p \Theta_o + U_M^2/2} 100\% \quad (20)$$

where N denotes the electric power supplied to each plate separately. During the entire experiment the



$$\begin{aligned} 55P61 \text{ and } 55P31 &- \theta, \overline{u_2^2}, \overline{u_3^2}, \overline{v^2}, \overline{u_2 v} \\ 55P61 \text{ and } 55P71 &- \overline{u_1^2}, \overline{u_2^2}, \overline{u_1 u_2} \end{aligned}$$

FIG. 3. The block diagram of the hot-wire setup.

parameter H did not exceed 1.86 which allowed us to rank this type of flow with the family of slightly nonisothermal flows, and justified the assumption of constant fluid density. All the measurements, taken at the mean-flow velocity $U_M = 11 \text{ m s}^{-1}$, were performed in a number of control planes $x_1 = \text{const}$ perpendicular to the wake axis and were within the limits $6t < x_1 < 16t$

4. EXPERIMENTAL RESULTS

4.1. Mean velocity and temperature evolution

The mean velocity and temperature distributions corresponding to the maximum value of flow-overheat parameter H and determined in consecutive control planes $x_1 = \text{const}$ have been presented in Fig. 4 in nondimensional form

$$F(\eta) = 2 \frac{U_{av} - U_1}{U_{1max} - U_{1min}}$$

$$F(\eta) = 2 \frac{\Theta - \Theta_{av}}{\Theta_{max} - \Theta_{min}}$$

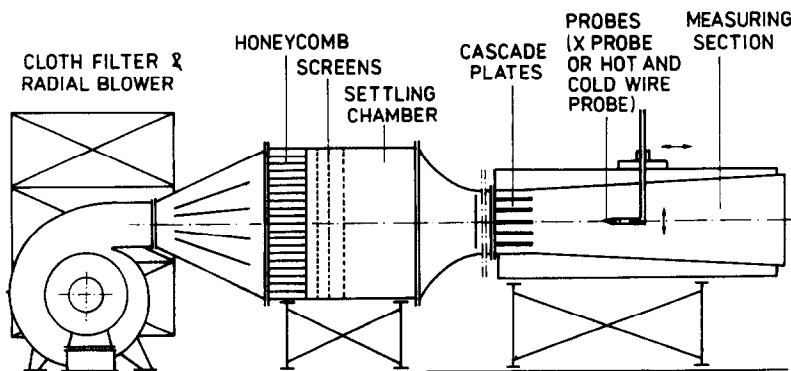


FIG. 2. The scheme of the experimental facility.

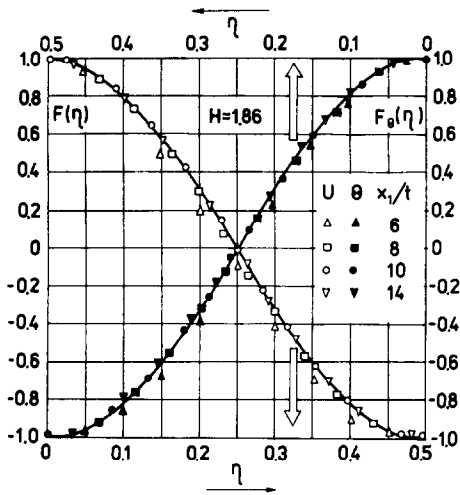


FIG. 4. The normalized mean velocity and temperature distributions for $H = 1.86$.

where the arithmetic average values (see Fig. 1) are

$$U_{av} = 0.5(U_{1max} + U_{1min}) \quad (21)$$

$$\Theta_{av} = 0.5(\Theta_{max} + \Theta_{min}).$$

Figure 4 reveals excellent agreement between the experimental data and the theoretical function $F = F_\theta = \cos 2\pi\eta$ given by equation (13) except for the nearest distance $x_1 = 6t$ considered here, where the velocity as well as the temperature profiles have not yet achieved their universal shape independent of the streamwise coordinate x_1 . Starting from the location $x_1 = 8t$ the arithmetic average values U_{av} and Θ_{av} become equal to the quantities U_M and Θ_M defined by equations (1) and (2), so that the mean velocity and temperature scales may be identified with

$$U^* = 0.5(U_{1max} - U_{1min})$$

$$\Theta^* = 0.5(\Theta_{max} - \Theta_{min}).$$

The downstream evolution of mean velocity and temperature fields may be characterized by parameters

$$\beta(x_1) = \frac{U_{1max} - U_{1min}}{2U_M}; \quad \beta_\theta(x_1) = \frac{\Theta_{max} - \Theta_{min}}{2\Theta_M}$$

which at the distance $x > 8t$ may be expressed in the form

$$\beta(x_1) = U^*/U_M; \quad \beta_\theta(x_1) = \Theta^*/\Theta_M.$$

At the distance $x_1 > 8t$ the functions $\beta(x_1)$ and $\beta_\theta(x_1)$ are represented in log-log coordinates (Fig. 5) by the straight lines with the slopes κ and κ_θ , respectively, which verifies the power-law relations used to describe the decay of mean velocity and temperature scales. It is interesting to note that within the experimental error the exponent κ is practically independent of flow overhear, while the exponent κ_θ seems to be a slightly increasing function of parameter H .

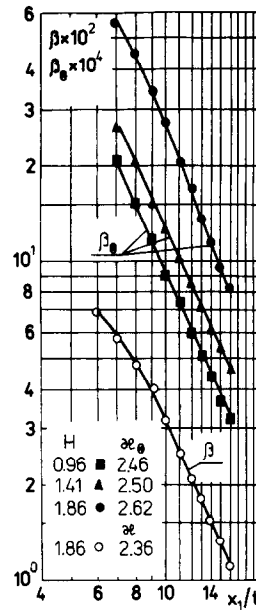


FIG. 5. The decay of nonuniformity parameters of mean velocity and temperature fields.

4.2. The decay of turbulent quantities

The turbulence structure in a cascade-wake-flow shows a high degree of anisotropy. According to experimental data $\overline{u_1^2}$ and $\overline{u_2^2}$ components of turbulent normal stresses are of the same order of magnitude while the remaining component $\overline{u_3^2}$ is evidently smaller than the former ones. It is also interesting to note that only the $\overline{u_2^2}$ component increases slightly with the growth of flow overhear, especially in the near-flow region. This tendency has also been observed by Kühn in a similar type of flow.

The exemplary lateral distributions of normal $\overline{u_1^2}$ and shear $\overline{u_1 u_2}$ Reynolds stresses normalized by their maximum values ($\overline{u_1^2}_{max}$ and $(\overline{u_1 u_2})_{max}$) have been presented in Fig. 6. Except for the nearest station

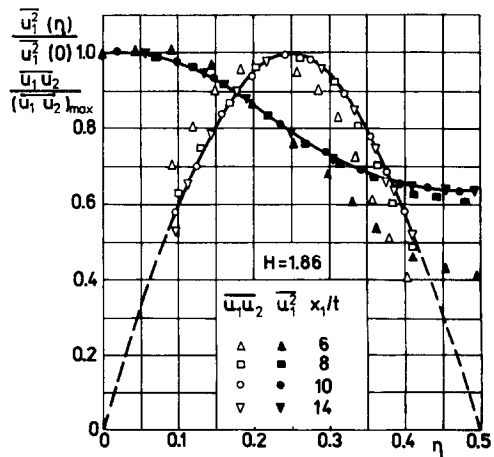


FIG. 6. The normalized distributions of the normal and shear stresses for $H = 1.86$.

$x_1 = 6t$ the empirical results seem to group fairly well about the common curves, which in the case of shear stresses may be approximated by equation (14a). The experimental scatter of the results is, however, evidently greater than that shown in Fig. 4 for mean quantity distributions. It may be attributed partly to the lower measuring accuracy and partly to the fact that turbulence quantities, in contrast to the mean ones, reveal their universal profiles in a considerably later stage of decay.

The evolution of normal turbulent stresses $\overline{u_i^2}$ measured in two control planes $x_2 = 0$ and $x_2 = t/2$ is shown in Fig. 7. It is easy to see that whereas the curves corresponding to $x_2 = 0$ linearize themselves in a log-log plot at a comparatively early stage, the ones determined in the plane $x_2 = t/2$ take their rectilinear character at a considerably greater distance from the plates. This phenomenon is probably caused by the intense mixing of two separate boundary layers flowing down from the adjacent plates of the cascade and merging finally together in the plane $x_2 = t/2$. At the distance approximately $x_1 = 10t$ all the curves discussed above become almost parallel, confirming the power-law dependence $u_i^{*2} \sim x_1^{-2k}$ expressed by equation (15), where $k_1 = k_2 = k_3 = k$.

In Fig. 7 the decay of turbulent shear stress normalized by U_M^2 has also been shown. For comparison a straight line with the slope k_{12} calculated from equation (17) is also plotted. Since $k_{12} > 2k_1$, one

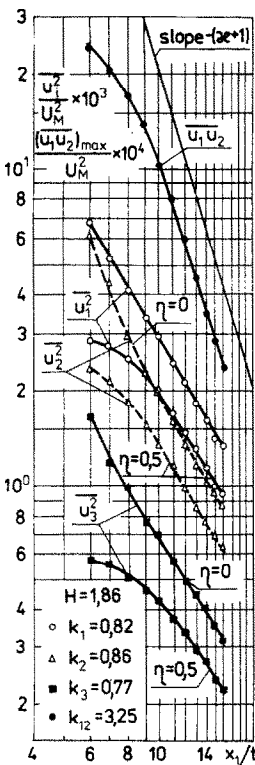


FIG. 7. The downstream evolution of the normal and shear turbulent stresses.

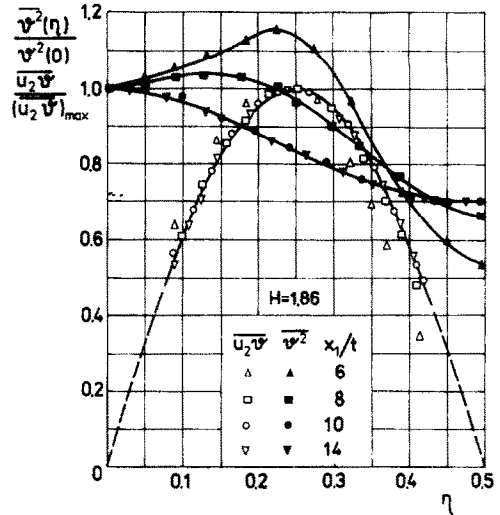


FIG. 8. The normalized distributions and turbulent heat-flux for $H = 1.86$.

can see that according to the previous predictions turbulent shear stress decays in the downstream direction more rapidly than the normal ones.

In nonisothermal flows the velocity fluctuations are accompanied with the random fluctuations of temperature. The lateral distributions of $\overline{\vartheta^2}(\eta)/\overline{\vartheta^2}(0)$ and $\overline{u_2\vartheta}/(\overline{u_2\vartheta})_{\max}$ have been presented in Fig. 8 for the maximum value of parameter $H = 1.86$. In the near-flow region one can observe the characteristic maxima of $\overline{\vartheta^2}(\eta)$ ($\eta \approx 0.22$ at $x_1 = 6t$) which move towards the wake axis with the growth of coordinate x_1 . It is the effect of warmer boundary layers flowing down from the plates and the intense transverse heat diffusion which tends to flatten the profiles of temperature fluctuations in a far-flow region.

Turbulent heat flux is expressed here by the correlation $\overline{u_2\vartheta}$. Experimental results of its lateral distributions normalized by the maximum value $(\overline{u_2\vartheta})_{\max}$ show a rather good agreement with the theoretical curve given by equation (14b) except for the near-flow region.

By analogy with Fig. 7 demonstrating the streamwise evolution of Reynolds stresses, Fig. 9 presents the decay of temperature fluctuations $\overline{\vartheta^2}$ corresponding to the maximum flow overheat and determined in two control planes $x_2 = 0$ and $x_2 = t/2$. Starting from the distance $x_1 \approx 10t$ both the curves plotted here in the log-log coordinates become mutually parallel straight lines with the slope $2k_3 \approx 1.2$, practically independent of parameter H .

Evolution of the maximum values of $(\overline{u_2\vartheta})_{\max}$ have also been illustrated in Fig. 9, this time for the various flow-overheat parameters. All the curves plotted here exhibit the rectilinear character for $x_1 > 10t$ which proves the validity of the power-law relation $\overline{u_2\vartheta} \sim x_1^{-k_{2\vartheta}}$ with the exponent $k_{2\vartheta}$ depending slightly on the value of parameter H .

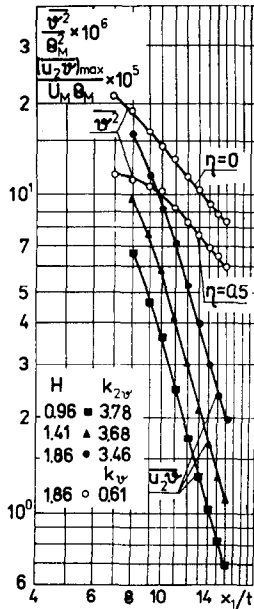


FIG. 9. The decay of temperature fluctuations and maximum lateral heat flux.

4.3. Eddy diffusion coefficients and turbulent Prandtl number

Experimental data presented before enable us to determine both the coefficients of eddy viscosity ν_T and turbulent heat diffusion a_T . They may be calculated from the definitions given by equations (5) and (6) using measured values of correlations $\overline{u_1 u_2}$ and $\overline{u_2 \vartheta}$ as well as the quantities U_1 and Θ of the mean flow. According to the usual predictions both these coefficients appear to have nearly constant values in the wake cross-sections being at the same time the inversely proportional functions of the streamwise coordinate x_1 (Fig. 10a).

The turbulent Prandtl number obtained as the ratio of experimentally determined transport coefficients ν_T and a_T has been confronted in Fig. 10b with the values calculated from equation (19) derived for the semi-

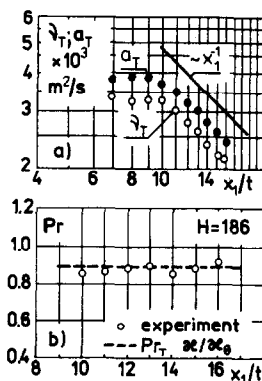


FIG. 10. The downstream evolution of: (a) eddy viscosity ν_T and heat diffusion a_T coefficients; (b) turbulent Prandtl number Pr_T .

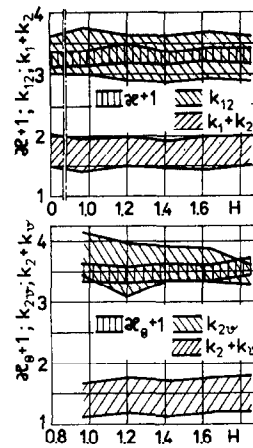


FIG. 11. The graphical verification of relations (17).

preserving region of the cascade-wake-flow. As can be seen, the compared results show the surprisingly good agreement, indicating at the same time that the turbulent Prandtl number has a constant value in the entire semi-preserving flow region.

5. CONCLUDING REMARKS

The experimental data presented above have confirmed the existence of the semi-preserving region in a far ($x > 10t$) nonisothermal cascade-wake-flow. All the characteristics velocity and temperature scales, different for the mean and turbulent motions show, in this region, the power-law dependence upon the streamwise coordinate x_1 , with the power indices which, according to Fig. 11, fulfill the conditions

$$k_{12} = \kappa + 1 > 2\kappa, \quad k_{2\vartheta} = \kappa_{\Theta} + 1 > \kappa + \kappa_g$$

resulting from the transport equations of momentum and heat, respectively. It should be emphasized, however, that the idea of semi-preservation does not exclude the concept of self-similarity, which may be regarded as the final stage of the flow evolution at the extremely far distance behind the cascade plates.

It has been also shown that in order to find the turbulent Prandtl number there is no need to measure the correlations $\overline{u_1 u_2}$ and $\overline{u_1 \vartheta}$, but it suffices to determine the evolution of mean velocity and temperature fields. The relationship (19) derived on the basis of semi-preservation hypothesis seems to be accurate enough and enables us to determine the value of Pr_T in a simple way, without the use of hot-wire or LDA techniques.

REFERENCES

- O. R. Gran, Geschwindigkeite und Temperaturverteilung hinter einem Gitter bei turbulenter Strömung, *Z. angew. Math. Mech.* 16, 257-267 (1936).
- H. Sato, On the turbulence behind a row of parallel rods, *1st Japan National Congress for Applied Mechanics*, pp. 469-473 (1951).

3. H. Tamaki and K. Oshima, Experimental studies on the wake behind a row of heated parallel rods, *Proc. 1st Japan National Congress for Applied Mechanics*, pp. 459–464 (1951).
4. F. Klatt, Experimentelle Untersuchungen zur Struktur des turbulenten Strömungsfeldes im inhomogen Gebiet hinter ebenen Turbulenzgittern. *Beiträge zur theoretischen und experimenteller Untersuchung der Turbulenz*, pp. 115–158 Akademie-Verlag, Berlin (1976).
5. J. W. Elsner and J. Wilczyński, Evolution of Reynolds stresses in turbulent wake flows with longitudinal pressure gradients, *Rozpr. Inz.-Eng. Trans.* **24**, 699–711 (1976).
6. J. W. Elsner and J. Wilczyński, Eddy viscosity in accelerated and retarded cascade-wake flows, *Rozpr. Inz.-Eng. Trans.* **27**, 547–557 (1979).
7. T. Matsui, Cross flow through a row heated rods, *75-AM JSME B-9 Joint JSME-ASME Applied Mechanics Western Conference*, pp. 415–429 (1975).
8. W. Kühn, Untersuchungen zum turbulenten Wärmetransport in Abhängigkeit von der Grobstruktur der Turbulenz. *Forschungsarbeiten zur Strömungsturbulenz schriftenreihe des Zentralinstituts für Mathematik und Mechanik der Akademie der Wissenschaften der DDR*, pp. 123–189. Akademi-Verlag, Berlin (1979).
9. J. W. Elsner and J. Zieliński, Studium pól prędkości i temperatur za palisadą podgrzewanych ciał symetrycznych. *Mat. Sympozjum. Doświadczalne Badania Przepływów*, Częstochowa, pp. 95–107 (1974).
10. J. W. Elsner, A conception of semi-preserving region in cascade flow, *Fluid Dynamics Trans.* **6**, 135–153 (1971).

SEMI-PRESERVATION DE LA QUANTITE DE MOUVEMENT ET DU TRANSFERT THERMIQUE DANS LES ECOULEMENTS A SILLAGE EN CASCADE

Résumé—On présente l'idée de la semi-préservation dans les écoulements à sillage en cascade non isotherme. En opposition avec le concept de self-similitude, l'évolution des écoulements semi-préservés est décrite en termes d'échelles caractéristiques de vitesse et de température, séparées pour les mouvements moyen et turbulent. Les équations de quantité de mouvement et de l'énergie permettent de déduire les corrélations mutuelles entre les échelles individuelles et de dériver des formules simples pour le nombre de Prandtl turbulent Pr_t^* en fonction des paramètres de l'écoulement moyen seulement. Finalement les prédictions théoriques sont confrontées avec les données expérimentales des auteurs.

"QUASI-ERHALTUNG" VON IMPULS- UND WÄRMETRANSPORT IN NACHLAUFSTRÖMUNGEN HINTER SCHAUFELGITTERN

Zusammenfassung—In dieser Arbeit wird die Idee der Quasi-Erhaltung in nichtisothermen Nachlaufströmungen hinter Schaufelgittern vorgestellt. Die Entwicklung von quasi-erhaltenden Strömungen wird durch charakteristische Geschwindigkeits- und Temperaturmaßstäbe, getrennt nach Haupt- und Turbulenzbewegung, beschrieben. Die Transportgleichungen für Impuls und Wärme erlauben es, für die einzelnen Maßstäbe ineinander überführende Korrelationen herzuleiten. Dadurch läßt sich eine einfache Beziehung für die turbulente Prandtl-Zahl entwickeln, in der diese nur noch durch Terme der Hauptströmungsparameter ausgedrückt wird. Zuletzt werden die theoretischen Vorhersagen mit den experimentellen Daten des Autors verglichen.

НЕПОЛНАЯ АВТОМОДЕЛЬНОСТЬ ПЕРЕНОСА ИМПУЛЬСА И ТЕПЛА ВО ВЗАИМОДЕЙСТВУЮЩИХ СЛЕДАХ

Аннотация—Изложена концепция неполной автомодельности в неизотермических течениях, образованных каскадом следов. В отличие от автомодельного развития эволюция вниз по потоку течений с неполной автомодельностью полей описывается с помощью характерных масштабов скорости и температуры, различных для среднего и турбулентного движений. Уравнения переноса импульса и тепла позволяют установить непосредственную связь между масштабами и вывести простую формулу для турбулентного числа Прандтля, как функции только осредненных параметров. Приводится сравнение теоретических результатов с экспериментальными данными, полученными авторами.